Available online at www.sciencedirect.com
ScienceDirect
Sensors and Actuators B 127 (2007) 54–62
SENSORS AND ACTUATORS B CHEMICAL
www.elsevier.com/locate/snb

Wireless Joule nanoheaters

Christian Falconi [a,b,*], Arnaldo D'Amico [a,b], Zhong Lin Wang [c]

[a] *Department of Electronic Engineering, University of Tor Vergata, Via del Politecnico 1, 00133 Rome, Italy*
[b] *CNR IDAC, Via Fosso del Cavaliere 100, 00133 Rome, Italy*
[c] *School of Materials Science and Engineering, Georgia Institute of Technology, Atlanta, GA 30332-0245, USA*

Available online 5 July 2007

Abstract

In principle, biocompatible, wireless nanotransducers might be useful for many *in vivo* biomedical applications such as hyperthermia, thermal ablation, targeted drug delivery, and *in vivo* monitoring of physiological parameters. In this article, we theoretically study the possibility of applying ring-shaped wireless Joule nanoheaters as possible nanovectors for targeted drug delivery, hyperthermia, and thermal ablation. This examination may offer an approach for guiding practical experiments.

Keywords: Wireless nanotransducers; Wireless Joule nanoheaters; Targeted drug delivery; Nanorings; Zinc oxide nanostructures

1. Introduction

Nanotechnology opens the way to a new generation of nano-sized transducers for *in vivo* biomedical applications, such as targeted drug delivery, hyperthermia, thermal ablation, and *in vivo* monitoring of physiological parameters. In most cases transducers are physically connected to electronic circuits by wires; this, however, may not be the best strategy for biomedical applications which require very small devices. We recently observed that, in these cases, a wireless approach might be more convenient and should be systematically explored [1]; in fact, only a few wireless nanoactuators have been proposed. In particular, wireless nanoheaters can selectively damage target cells by heating (hyperthermia, or thermal ablation if the temperature is so high that cells are destroyed); based on this principle, magnetic nanoparticles [2–4] and gold nanoshells [5] have been used for killing cancer cells by thermal ablation. The potential of both magnetic nanoparticles (transducing the magnetic field into position) [4,6,7] and of gold nanoshells [8,9] for targeted drug delivery has also been investigated. Furthermore, there might be many other opportunities for wireless nanotransducers [1].

As to hyperthermia or thermal ablation, other wireless nanoheaters might be used; as to drug delivery, nanotransducers and therapeutics may be included in a special coating which should be broken-perforated-dissolved-melt upon excitation, thus releasing drugs in a selective, controlled, and accurate manner [1] (this is a generalization of the "photothermally induced" targeted drug delivery reported in [8,9]). In all cases, the selectivity (i.e. the ability to selectively deliver drugs or to heat only the target cells) may be obtained by focusing the exciting waves only in specific regions of the body and/or by properly functionalizing the coating so that it will preferentially bind to specific cells (for instance, attaching antibodies which only bind to specific molecules present on the surface of cancer cells). As an example, in this paper we study ring-shaped nanostructures which can be wirelessly excited by means of an electromagnetic field (wireless Joule nanoheater); as other wireless nanoheaters, these nanostructures could be useful for hyperthermia, thermal ablation, or targeted drug delivery. As a second example, an electromagnetic field may induce mechanical vibrations in piezoelectric nanostructures (nanopumps, nanoscissors, vibration nanoheaters, etc.) which could be useful in medical applications [1].

Wireless nanotransducers could also be used for *in vivo* monitoring of physiological parameters [1]. As an example, if we again consider an electromagnetically excited ring-shaped nanostructure, after the excitation is removed, the current in the ring will decay and re-irradiate an electromagnetic wave, eventually with characteristics related to a measurand [1]. In the same manner, if we again consider an electromagnetically excited piezoelectric nanostructure, after the excitation is removed, the mechanical vibrations will decay, re-irradiating an electromagnetic wave, eventually with characteristics related to a measurand [1] (viscosity, flow, etc.). Obviously, in the case of

* Corresponding author at: Department of Electronic Engineering, University of Tor Vergata, Via del Politecnico 1, 00133 Rome, Italy.
E-mail address: falconi@eln.uniroma2.it (C. Falconi).

0925-4005/$ – see front matter © 2007 Elsevier B.V. All rights reserved.
doi:10.1016/j.snb.2007.07.002

these "wireless nanosensors", obtaining a reasonable accuracy would require an accurate detection of the re-irradiated electromagnetic fields (we mention that the waves re-irradiated by different nanostructures, even with a random orientation, would still add along the direction of the linearly polarized exciting electromagnetic radiation); although different wireless sensors (e.g. see [10]) are being considered for other applications, the proposed wireless *nano*sensors might be best suited for *in vivo* monitoring of physiological parameters.

Beside wireless nanotransducers, different methods for applying nanotechnology to medicine are also being explored [11–17]; as an example, nanocells with a diameter smaller than 200 nm have been used as drug delivery systems in a successful attempt for combining traditional chemotherapy with anti-angiogenesis [17]. In general, a fundamental concern is the patient safety even after long-term exposure to the therapeutic nanoparticles (especially with reference to toxicity and to the risk of undesired aggregation and obstruction of blood vessels).

Recently, nanostructures which seem ideally suited for fabricating wireless nanotransducers for biomedical applications have been reported [18–21]: almost defect-free, self-assembled monocrystals of zinc oxide (ZnO). In fact, as to signal conversion, the geometries of these nanostructures (rings [19], helixes [20], etc.) permit an efficient electromagnetic wireless interaction; moreover, zinc oxide is piezoelectric. Additionally, these single-crystal nanostructures have excellent mechanical properties. Other advantages concerning the patient safety are also likely: zinc oxide is biocompatible and biosafe (i.e. non-toxic); besides, the unique geometries of zinc oxide nanostructures should, hopefully, prevent the obstruction of blood vessels; finally, once immersed in water, zinc oxide nanostructures are automatically dissolved after a few hours. As a possible application of the unique properties of these self-assembled ZnO nanostructures, wirelessly excited ZnO nanohelixes could selectively damage the target cells [1] (by heating or by inertial cavitation [22]) and could be automatically dissolved into the body after use (these are ideal characteristics for *in vivo* biomedical applications as zinc oxide is not toxic and there would be no self-aggregation risks).

In this paper we focus on wireless Joule nanoheaters. Since the electromagnetic-to-heat transduction process does not rely on the optical properties of the nanostructures, the addition of non-transparent coating layers does not necessarily degrade the signal conversion efficiency. In Section 2 we discuss some simplifying assumptions which will be used throughout this paper and we discuss an electrical model for wireless Joule heaters; this model is employed in Section 3 in order, first, to maximize the temperature difference between the nanoheater and the surroundings and, second, to estimate the extinction cross-section. Since heat transfer at nanoscale is extremely complex [23–29] an accurate, quantitative evaluation of the thermal resistance between a nanoring and the surroundings is, practically, impossible; however, in Section 4 we discuss a qualitative analysis which provides insight for the design of effective wireless Joule heaters. In Section 5 we discuss the potential use of wireless Joule nanoheaters for *in vivo* biomedical applications; although various techniques can be used for fabricating nanorings [31–33], in Section 6, as an example, we apply our analysis to the design of multi-shell (two layers) wireless Joule nanoheaters based on zinc oxide nanorings [19,21]. Preliminary conclusions are drawn in Section 7.

2. Electrical model for wireless Joule heaters

According to Faraday's law, alternating electromagnetic fields generate alternating electrical currents inside loop-shaped structures, as schematically shown in Fig. 1. Electrical currents produce heat due to the Joule effect (wireless Joule heaters); this wideband transduction mechanism does not require an exciting radiation with a high spectral purity. Although we are mainly interested in *nano*sized heaters, in this section we discuss an electrical model for toroidal wireless Joule heaters.

2.1. Toroidal geometry

We consider a simplified toroidal geometry characterized by r_0, radius of the tube, and R, radius of the torus (see Fig. 1 for a section of the toroidal ring). This choice allows to find very simple analytical relations and to focus on the very important role of the dimensionless aspect ratio ζ (see, for instance, the conclusions), which is defined as follows

$$\zeta = \frac{R}{r_0}. \tag{1}$$

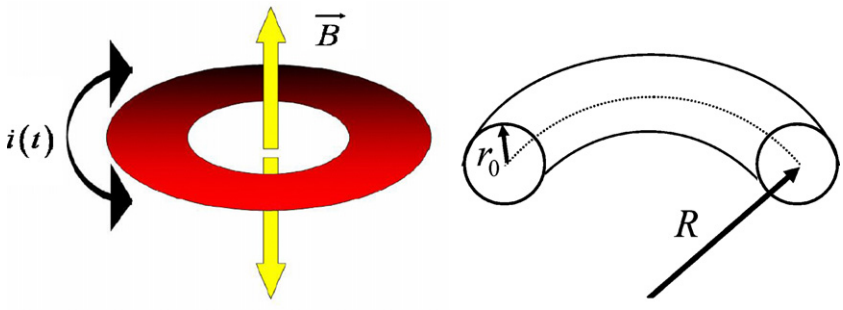

Fig. 1. Wireless generation of alternating currents in a nanoring and section of the simplified toroidal geometry.

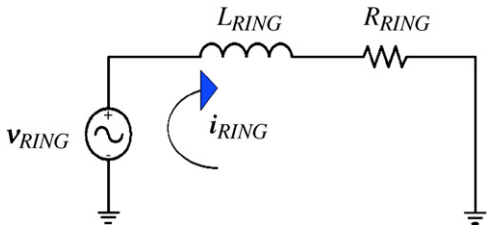

Fig. 2. Electrical model for the nanoring.

2.2. Wavelength assumption

We assume that the wavelength of the exciting radiation is much bigger than the diameter of the torus ($2R$). As a result, the magnetic field is approximately constant through the loop area; moreover, there is no need for distributed constant models. In practice, this assumption limits the maximum frequency of the exciting electromagnetic radiation.

2.3. Electrical insulation assumption

We assume that the nanoring is electrically insulated from the environment; in fact, even if the nanoring is surrounded by a relatively conducting material such as blood, at the frequencies of the electromagnetic excitation, blood is, in practice, an insulator.

2.4. Electrical model for wireless Joule heaters

Fig. 2 shows the resulting electrical model of the nanoring. Under the wavelength and the electrical insulation assumptions, the nanoring can be considered as an electrically small circular loop antenna in receiving mode [34]. According to Faraday's law,

$$|v_{\mathrm{RING}}(t)| = \left|\frac{\mathrm{d}\Phi_{\mathrm{B}}(t)}{\mathrm{d}t}\right|. \tag{2}$$

For simplicity, let us first consider a *linearly polarized* plane wave. At any given time instant, the intensity of the magnetic flux density is almost constant over all the loop area, A_{LOOP} (wavelength assumption); therefore, considering a sinusoidal magnetic flux density, B, we may write

$$\begin{aligned}\Phi_{\mathrm{B}}(t) &= \int_{S_{\mathrm{RING}}} \overrightarrow{B(t)}\,\overrightarrow{\mathrm{d}S} = B_0 \sin(2\pi f_0 t) A_{\mathrm{LOOP}} \cos(\varphi) \\ &= \mu H_0 \sin(2\pi f_0 t) A_{\mathrm{LOOP}} \cos(\varphi),\end{aligned} \tag{3}$$

where μ is the magnetic permeability of the material in which the nanoring is immersed, f_0 the frequency, φ the angle between the axis of the ring and the direction of the linearly polarized magnetic field, and B_0 and H_0 are the intensities of, respectively, the magnetic flux density and the magnetic field.

Substituting (3) into (2), we find

$$\begin{aligned}|v_{\mathrm{RING}}(t)| &= \left|\frac{\mathrm{d}\Phi_{\mathrm{B}}(t)}{\mathrm{d}t}\right| = \left|\frac{\mathrm{d}[\mu H_0 \sin(2\pi f_0 t) A_{\mathrm{LOOP}} \cos(\varphi)]}{\mathrm{d}t}\right| \\ &= 2\pi f_0 \mu H_0 A_{\mathrm{LOOP}} \left|\cos(2\pi f_0 t)\cos(\varphi)\right|.\end{aligned} \tag{4}$$

In the case of an incident plane wave, the voltage v_{RING} becomes [34]

$$|v_{\mathrm{RING}}(t)| = 2\pi f_0 \mu H_{Z0} A_{\mathrm{LOOP}} \left|\cos(2\pi f_0 t)\right|, \tag{5}$$

where H_{Z0} is the component of the magnetic field normal to the plane of the loop.

Taking into account the electrical equivalent circuit shown in Fig. 2, we find the fundamental relations for the average Joule power dissipated in the nanoring, P_{JOULE}, and the temperature difference between the nanoheater and the surroundings, ΔT

$$\begin{aligned}P_{\mathrm{JOULE}} &= R_{\mathrm{RING}} \frac{2[\pi f_0 \mu H_{Z0} A_{\mathrm{LOOP}}]^2}{R_{\mathrm{RING}}^2 + (2\pi f_0 L_{\mathrm{RING}})^2}, \\ \Delta T &= R_{\mathrm{TH}} P_{\mathrm{JOULE}} = R_{\mathrm{TH}} R_{\mathrm{RING}} \frac{2[\pi f_0 \mu H_{Z0} A_{\mathrm{LOOP}}]^2}{R_{\mathrm{RING}}^2 + (2\pi f_0 L_{\mathrm{RING}})^2},\end{aligned} \tag{6}$$

where R_{TH} is the thermal resistance between the nanoring and the surrounding environment. Although we only consider the Joule effect, other absorption mechanisms and, more in general, all dissipation processes which selectively heat the nanoring are favorable.

If we neglect the radiation resistance (loop antennas with electrically small perimeters generally have radiation resistances much smaller than their loss resistances [34]), in the fundamental relations (6), the loop area, the electrical resistance and the inductance of the toroidal ring may be approximated as follows

$$\begin{aligned}&A_{\mathrm{LOOP}} \simeq \pi R^2, \qquad R_{\mathrm{RING}} \simeq 2\rho \frac{R}{r_0^2} = 2\rho\zeta^2 \frac{1}{R}, \\ &L_{\mathrm{RING}} \simeq \mu R \left[\ln(8\zeta) - \frac{7}{4}\right].\end{aligned} \tag{7}$$

3. Frequency, electrical resistivity, and extinction cross-section

In this section, *assuming that parasitic capacitances are negligible*, we determine the frequency and the electrical resistivity which maximize ΔT; afterwards, we compute the extinction cross-section of wireless Joule heaters.

3.1. Frequency

Assuming that parasitic capacitances are negligible, we have found the expression for ΔT (6); we may now consider the following three possibilities

$$\begin{aligned}&\text{(i)} R_{\mathrm{RING}} \gg 2\pi f_0 L_{\mathrm{RING}}, \qquad \text{(ii)}\ R_{\mathrm{RING}} \simeq 2\pi f_0 L_{\mathrm{RING}}, \\ &\text{(iii)} R_{\mathrm{RING}} \ll 2\pi f_0 L_{\mathrm{RING}}.\end{aligned} \tag{8}$$

Correspondently, we may simplify the expression for ΔT as

follows

$$\text{(i)}\ \Delta T \simeq R_{\mathrm{TH}} \frac{2[\pi f_0 \mu H_{Z0} A_{\mathrm{LOOP}}]^2}{R_{\mathrm{RING}}} \propto [f_0]^2,$$

$$\text{(ii)}\ \Delta T \simeq R_{\mathrm{TH}} \frac{2[\pi f_0 \mu H_{Z0} A_{\mathrm{LOOP}}]^2}{2R_{\mathrm{RING}}} \propto [f_0]^2,$$

$$\text{(iii)}\ \Delta T \simeq R_{\mathrm{TH}} R_{\mathrm{RING}} \frac{2[\pi \mu H_{Z0} A_{\mathrm{LOOP}}]^2}{(2\pi L_{\mathrm{RING}})^2} \propto [f_0]^0. \quad (9)$$

In conclusion, in the first two cases ΔT is proportional to f_0^2, while in the third case it does not depend on f_0. In general, it is therefore convenient to use the maximum possible f_0; if we consider the limit imposed by the wavelength assumption, this corresponds to use

$$f_0 = f_{0,\max} = \frac{ac}{2R}, \quad a \ll 1, \quad (10)$$

where the dimensionless constant a is the ratio between the diameter of the ring and the wavelength.

3.2. Resistivity

In theory changing the electrical resistivity corresponds to, somehow, changing the material (including its thermal properties) so that there may be some correlation between the resistivity and the thermal resistance in (6). Although an accurate thermal analysis is virtually impossible (see later), we expect that the ring resistance depends on the electrical resistivity much more than the thermal resistance; it is therefore appropriate to neglect the dependence of the thermal resistance on the electrical resistivity.

If the only parameter which depends on the electrical resistivity is R_{RING}, ΔT is maximum when

$$[R_{\mathrm{RING}} = 2\pi f_0 L_{\mathrm{RING}}] \Rightarrow \rho = \frac{\pi ac \mu R[\ln(8\zeta) - (7/4)]}{2\zeta^2}, \quad (11)$$

where we have used (10); we stress that, in practice, the matching condition (11) must be satisfied by taking into account both the existence of cracks in very metal thin films and the skin effect (see Section 6). We may now simplify the *maximum* ΔT

$$\Delta T_{\max} = R_{\mathrm{TH}} \frac{[\pi f_0 \mu H_{Z0} A_{\mathrm{LOOP}}]^2}{R_{\mathrm{RING}}}. \quad (12)$$

We observe that, if we keep constant both the resistivity and the aspect ratio ζ, the ring resistance is inversely proportional to R (see (7)); however, if we tune the resistivity according to (11), the ring resistance is (see (10))

$$R_{\mathrm{RING}} = 2\pi f_0 L_{\mathrm{RING}} = \pi ac \left(\mu \left[\ln(8\zeta) - \frac{7}{4} \right] \right) \quad (13)$$

which, for a constant aspect ratio ζ is constant and, in particular, does not depend on R. This observation will be useful for estimating the dependence of the maximum ΔT on the geometry of the torus.

According to (11), the optimal resistivity depends on both the radius of the torus and the aspect ratio ζ. If, as an example, we consider free air, Fig. 3 shows that for some geometries of the torus, an unrealistic optimal electrical resistivity would be required (notice that, for simplicity, unrealistic geometries such as [$R = 1$ nm, $\zeta = 1000$] are also included in the graph).

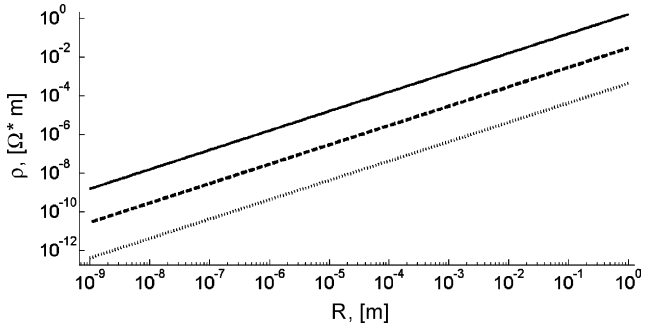

Fig. 3. Optimum (theoretical) resistivity as a function of the radius for different aspect ratios: $\zeta = 10$ (dotted line), $\zeta = 100$ (dashed line), $\zeta = 1000$ (solid line).

3.3. Extinction cross-section

If, for simplicity, we assume that the axis of the nanoring and the direction of the magnetic field are parallel (see later for a discussion), the extinction cross-section of a single wireless Joule heater is

$$\sigma_{\mathrm{ext}} = \frac{P_{\mathrm{JOULE}}}{((1/2)ZH_0^2)} = \frac{2\pi^2 f_0^2 \mu^2 A_{\mathrm{LOOP}}^2}{ZR_{\mathrm{RING}}}. \quad (14)$$

With the design choices (10) and (11), the optimum (i.e. maximum for a given geometry) extinction cross-section is

$$\sigma_{\mathrm{ext}} = \frac{\pi^3 ac \mu R^2}{2Z[\ln(8\zeta) - (7/4)]} \quad (15)$$

which, for a constant aspect ratio, is proportional to the area of the ring, πR^2. Fig. 4 shows in a log–log scale the optimum (theoretical) extinction cross-section of a wireless Joule nanoheater as a function of the radius for an aspect ratio $\zeta = 10$ when the dimensionless constant a is equal to 0.28 (though this is an extreme case, the extinction cross-section for different values of a can be easily determined from this figure by taking into account the lin-

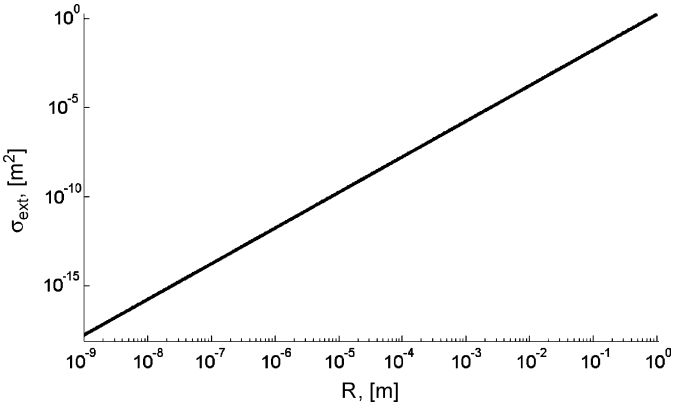

Fig. 4. Optimum (theoretical) extinction cross-section of a wireless Joule nanoheater as a function of the radius for an aspect ratio $\zeta = 10$ for the dimensionless constant a equal to 0.28.

ear dependence of σ_{ext} on a). Finally, we observe that, as evident from (15), the optimum extinction cross-section is only weakly dependent on the aspect ratio ζ.

4. Thermal resistance

In order to estimate the temperature difference between the nanoheater and the surroundings when the design rules found in the previous section are satisfied, we must determine the thermal resistance between the ring-shaped wireless heater and the surroundings; clearly, for *in vivo* biomedical applications, only wireless *nano*heaters may be considered. Since at nanoscale the classic heat transfer theory is no longer valid [23], an accurate heat transfer analysis of even the simplest possible wireless Joule *nano*heaters is far beyond what is today possible. Numerical simulations would also be problematic; in fact, in molecular dynamics simulations [24,25] each molecule must be independently considered; as a result, among the three modes of heat transfer, only heat conduction (in very small volumes) can be investigated. Beside computational difficulties, molecular dynamics also require an accurate knowledge of all the relevant intermolecular interactions, which would not be easy for our target application.

Though the complexity of nanoscale heat transfer impedes a quantitative estimation of the thermal resistance R_{TH} between the heater and the surroundings, it is possible to gain insight for the design of effective wireless Joule nanoheaters. In fact, if we consider heat conduction perpendicular to an interface, reflection of thermal energy waves (i.e. phonon backscattering) may occur, thus limiting heat transfer; equivalently, at the interface between two materials there is a thermal boundary resistance (also known as Kapitza resistance) which is inversely proportional to the area of the interface. Although in macroscopic systems the role of the thermal boundary resistance is generally negligible, at nanoscale, the Kapitza resistance often dominates the thermal resistance; as an example, in [26] a nanotube was heated by a laser beam and an extremely high Kapitza resistance was derived from the exponential decay of the nanotube temperature; we mention that [26] is one of the very few papers containing experimental results on the Kapitza resistance at a solid–liquid interface, which is analogous to our target application (the role of the Kapitza resistance at nanoscale is also discussed in, for instance [27–29]). In practice, at the interface between two materials X and Y, we may consider a (Kapitza) conduction thermal resistance

$$R_{TH,conduction} = \frac{1}{\kappa_{X,Y} A}, \tag{16}$$

where $\kappa_{X,Y}$ is the interface thermal conductivity per unit area and depends on the two materials X and Y.

For generality, let us consider a multi-shell structure constituted by the nanoring (0th layer) and by N coating layers (e.g. including therapeutics); for simplicity, the surroundings (e.g. blood) are referred to as the $(N+1)$th layer. As an example, Fig. 5 shows the section of a multi-shell three layers coated nanoring.

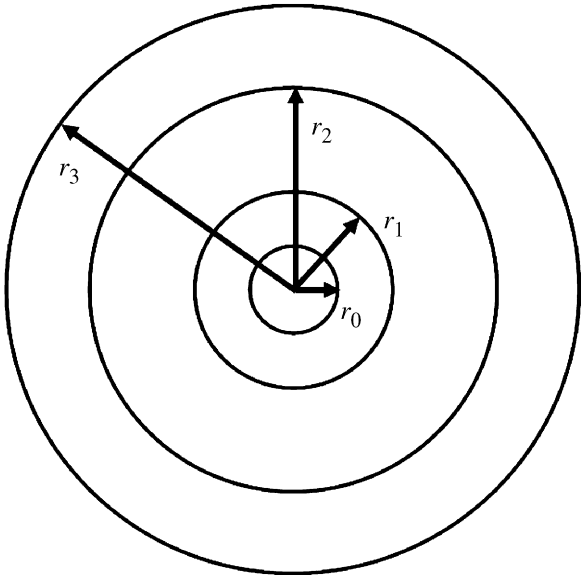

Fig. 5. Section of a multi-shell three layers coated nanoring.

The thermal resistance between the (internal) nth layer and the surroundings (e.g. blood) is

$$\forall n = 0, 1, 2, \ldots, (N-1) \rightarrow R_{TH,n} = \sum_{i=n}^{N-1} \frac{1}{\kappa_{i,i+1} A_i} + R_{TH,N},$$

$$A_i = (2\pi R)(2\pi r_i), \tag{17}$$

where A_i is the area of the interface between the ith layer and the $(i+1)$th layer and $R_{TH,N}$ is the thermal resistance between the outer coating layer and the surroundings,

$$R_{TH,N} = \left(\frac{1}{\kappa_{N,N+1} A_N}\right) \propto \frac{1}{A_N}, \quad A_N = (2\pi R)(2\pi r_N). \tag{18}$$

If we keep constant all the aspect ratios $[\Re_1 = (r_1/r_0), \ldots, \Re_N = (r_N/r_0)]$, it is easy to find

$$\forall n = 0, 1, 2, \ldots, N \rightarrow R_{TH,n} \propto \frac{1}{r_0 R}. \tag{19}$$

If we assume that the induced electrical current is flowing in an inner layer, the maximum ΔT between the nth coating layer and the surroundings will be

$$\Delta T_{max,n} = R_{TH,n} \frac{[\pi f_0 \mu H_0 A_{LOOP} |\cos(\varphi)|]^2}{R_{RING}}. \tag{20}$$

For fixed aspect ratios ζ and $[\Re_1, \ldots, \Re_N]$, if we consider that

$$R_{TH,n} \propto \frac{1}{r_0 R} = \frac{\zeta}{R^2}, \qquad f_0 = f_{0,max} = \frac{ac}{2R} \propto \frac{1}{R},$$

$$A_{LOOP} = \pi R^2 \propto R^2, \qquad R_{RING} \propto R^0 \tag{21}$$

the maximum ΔT (20) does not depend on the radius of the torus. Additionally, if we neglect the weak logarithmic dependence of the inductance L_{RING} on the aspect ratio ζ, the maximum ΔT is proportional to ζ.

In conclusion, assuming that the Kapitza resistance dominates the thermal resistance between the ring-shaped nanoheater

and the surroundings, and keeping all the aspect ratios constant, downscaling does not degrade the maximum possible ΔT (an important result in view of *in vivo* biomedical applications which require very small wireless Joule heaters). Furthermore, *ceteris paribus*, nanorings with high aspect ratios ζ may lead to higher ΔT.

5. Wireless Joule nanoheaters as possible nanovectors for *in vivo* biomedical applications

In this section we discuss both issues and opportunities concerning the possible use of wireless Joule heaters for *in vivo* biomedical applications. We stress that, though we have only considered the Joule effect, other absorption mechanisms and, more in general, all dissipation processes which selectively heat the nanoring are favorable (including, eventually, the absorption mechanisms described in [31]).

5.1. Dimensions of the transducers

Only nanosized wireless Joule heaters are suitable for *in vivo* biomedical applications. In particular, depending on their dimensions, drug delivery devices may be injected into tissues (<200 μm), inhaled (<100 μm), or released into circulation (<10 μm) [14]. In the case of wireless Joule nanoheaters it is also important to selectively heat only the target regions of the human body; for this reason the wavelength of the exciting radiation should preferably belong to the so called "water window" (the human body is relatively transparent to radiations within this bandwidth, approximately from 800 nm to 1200 nm). Since the wavelength of the exciting radiation should be much bigger than the diameter of the torus ($2R$), only nanorings with a diameter below a few hundreds nanometers may be considered.

5.2. Internal and outer coating layers

In order to take advantage of wireless Joule nanoheaters for targeted drug delivery, hyperthermia, or thermal ablation, an electromagnetic radiation with an acceptable intensity must produce a significant temperature increase. Clearly, this requires high thermal resistances between the nanoheaters and the surroundings. As evident from (17), if necessary, high thermal resistances between an *internal* layer and the surroundings may be obtained by using *nanolaminates* [29] (i.e. alternating layers constituted by materials which have a very low interface thermal conductivity); clearly, only biocompatible and biosafe materials should be considered. However, the ΔT between the outer layer and the surroundings only depends on $R_{TH,N}$ (see (18)). In practice, the outer layer plays a special role as, for hyperthermia, this layer establishes the ΔT, and, for drug delivery, it must release the therapeutics after the nanoheater is activated.

5.3. Orientation of the nanorings

For a linearly polarized magnetic field, in order to estimate the maximum possible ΔT, we may consider the magnetic field almost aligned with the axis of the nanoring. If many exciting electromagnetic waves can be repeatedly used, this simplification may be acceptable; in fact, each nanoring in the blood may freely move and therefore its axis will, soon or later, be aligned with the magnetic field. Since the nanoring has a very small thermal time constant (because of its very small mass), the maximum ΔT will be reached before the nanoring will further significantly change its position. Similar considerations apply to the general case of an incident plane wave.

5.4. Smart self-activated wireless drug delivery nanodevice

The dependence of the Joule power on the ring resistance might, in principle, allow a "smart" self-activation of the nanoheaters. In fact, if the ring resistance is dominated by the resistance of the outer coating layer, R_X, a proper variation of R_X (e.g. due to the interaction with a target cell) may enable or disable the nanoheater.

6. Case study: wireless Joule nanoheaters based on zinc oxide nanorings

Although, as we have discussed, a theoretical estimation of the performance of wireless Joule nanoheaters is impossible due to the limited knowledge on nanoscale heat transfer, our theoretical analysis may be used for designing high efficiency wireless Joule nanoheaters. As an example, in this section we describe the design of multi-shell (two layers) wireless Joule nanoheaters based on ZnO nanorings; in fact, among many other methods for fabricating nanorings [30–33], these ZnO nanostructures have interesting properties for *in vivo* biomedical applications.

ZnO nanorings are self-assembled single-crystal loop-shaped nanostructures; Fig. 6 shows the growth process and the corresponding experiment showing the initiation and formation of the single-crystal nanoring via self-coiling of a polar nanobelt [19]; the nanoring is initiated by folding a ZnO nanobelt [18] into a loop with overlapped ends driven by long-range electrostatic interactions among the polar charges; short-range chemical bonding stabilizes the coiled ring structure, and the spontaneous self-coiling of the nanobelt is driven by minimizing the energy contributed by polar charges, surface area, and elastic deformation [19]. The single-crystal nature of these nanostructures explains their excellent mechanical properties; for instance, Fig. 7 shows a series of AFM images which illustrate the manipulation of a ZnO nanoring with a high aspect ratio; although the strain stored within the nanoring is extremely large, no fracture occurs [21]. Additionally zinc oxide is biosafe (i.e. non-toxic) and biocompatible. Furthermore, ZnO nanorings may have high aspect ratios ζ (see Fig. 7), which is beneficial for different reasons: first, *ceteris paribus*, ΔT is proportional to the aspect ratio; second, the undesired aggregation of nanorings with high aspect ratios seems unlikely (one of the main concerns for the injection of nanovectors in the body [15] is their possible aggregation which might lead, over long time periods, to obstruction of the blood vessels).

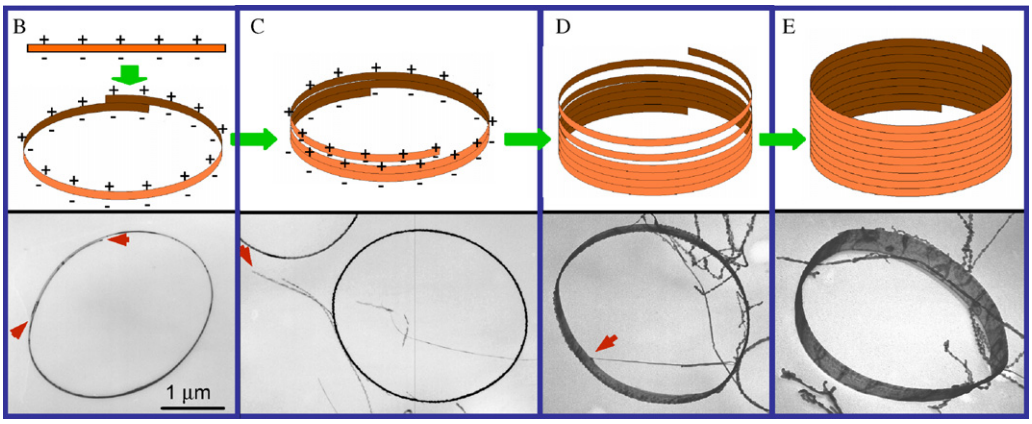

Fig. 6. Growth process and corresponding experiment showing the initiation and formation of the single-crystal nanoring via self-coiling of a polar nanobelt (see [19]).

6.1. Geometry

So far reported zinc oxide nanorings have typical radii of ∼400 nm to ∼2 μm, thicknesses of ∼10 nm to ∼30 nm; the width of the shell is up to ∼1 μm, depending on the number of loop-by-loop windings of the nanobelt [19]. In order to obtain an high aspect ratio ζ, it is better to keep as small as possible the number of windings. In order to use exciting radiations within the "water window", only nanorings with extremely small diameters should be considered; for instance, if we consider a wavelength equal to 1.2 μm and $a = 0.15$, an acceptable nanoring should have the radius of the torus smaller than 90 nm (the smallest reported ZnO nanorings have a radius equal to 400 nm [19]); as it is clear from Fig. 3 very small nanorings have optimal resistivities which are orders of magnitude smaller than the resistivity of even heavily doped zinc oxide crystals (see [35] for an extensive discussion of the resistivity of both single crystal and polycrystalline zinc oxide). However, if we cover the natu-

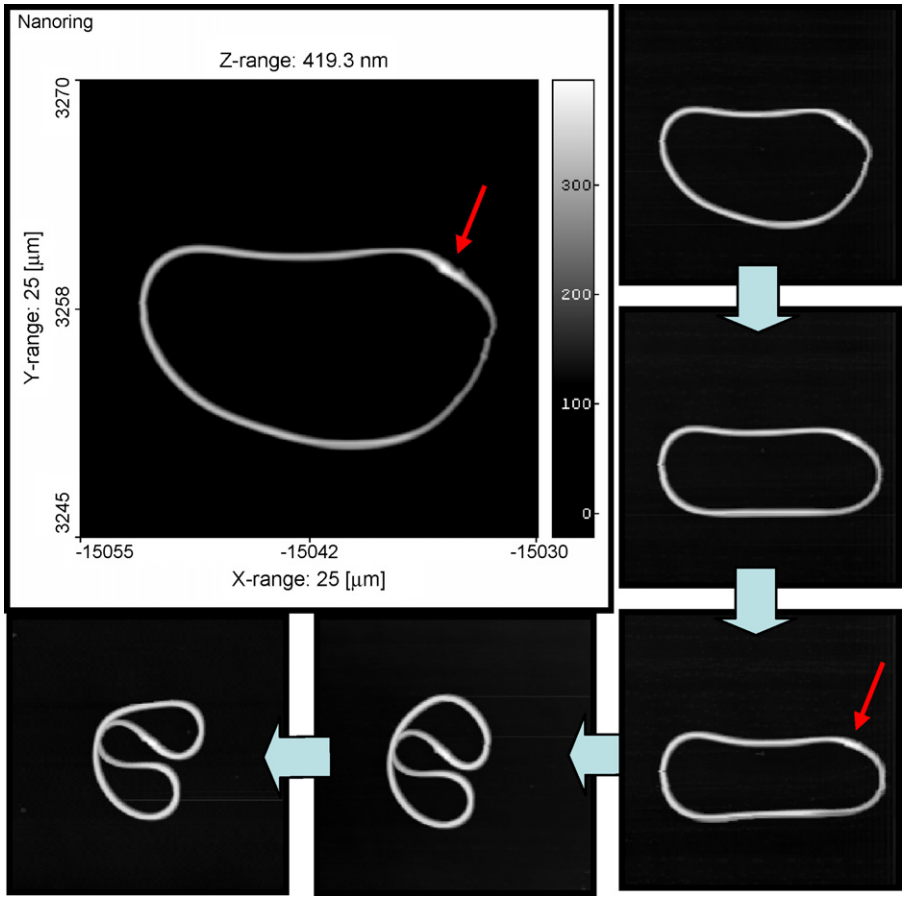

Fig. 7. Series of AFM images showing the manipulation of a ZnO nanoring with a high aspect ratio (see [21]).

ral zinc oxide nanoring with a thin metal layer, the *equivalent* resistivity of the coated nanoring may be tuned by modifying the thickness of the coating metal layer.

As an example, let us consider a wavelength equal to 1.2 μm, $a = 0.15$, and an hypothetical *equivalent* toroidal nanoring having the radius of the torus, R, and the radius of the tube, r_0, as follows

$$R = 90\,\text{nm}, \quad r_0 = 10\,\text{nm}. \tag{22}$$

If this *equivalent* toroidal nanoring is immersed in the human blood ($\mu_r \simeq 1$; at these high frequencies $\varepsilon_r \simeq 5$), the optimal resistivity is equal to $1.1 \times 10^{-7}\,\Omega\,\text{m}$. If we consider a uniform gold coating ($\rho_{Au} \simeq 1.7 \times 10^{-8}\,\Omega\,\text{m}$) and we neglect the contributions of the zinc oxide nanoring to the electrical conduction, the thickness of the coating layer ($t_{Au} = r_1 - r_0$) which gives the optimal ring resistance is easily determined as follows

$$\left[\frac{\rho_{Au}}{\pi(r_1^2 - r_0^2)} = \frac{\rho}{\pi r_0^2}\right] \Rightarrow t_{Au} = r_0\left(\sqrt{\frac{\rho_{Au}}{\rho} + 1} - 1\right) \simeq 0.74\,\text{nm}. \tag{23}$$

Such a small thickness is, clearly, an underestimation, as, in practice, both the presence of cracks in thin metal films and the skin effect should be considered. The extinction cross-section (with the design choices (10) and (11)) may be computed according to (15) as follows

$$\sigma_{ext} = \frac{\pi^3 ac\mu R^2}{2Z[\ln(8\zeta) - (7/4)]} = 7.5 \times 10^{-15}\,\text{m}^2. \tag{24}$$

In conclusion, if a metal coating is used, we expect that the self-assembled zinc oxide nanoring mainly determines the geometry and the mechanical robustness of the nanoheater, while the metal layer determines the ring resistance so that the *maximum* ΔT may be achieved. Though, obviously, these results need an experimental confirmation, the proposed analysis might be useful for a first design of efficient loop-shaped wireless Joule nanoheaters.

6.2. Thermal resistance between the nanoring and the surroundings

Unfortunately, measured interfacial thermal conductivities per unit area between solids and liquids have been reported only for very few cases [26–28] so that even a rough estimation of the interfacial thermal conductivity is impossible and *ad hoc* experiments are required.

7. Conclusion

Here we have theoretically studied the potential of wireless nanotransducers for biomedical applications such as targeted drug delivery, hyperthermia, thermal ablation, and *in vivo* monitoring of physiological parameters. In particular, we have focused on wireless Joule nanoheaters. Although the limited knowledge on nanoscale heat transfer make a theoretical characterization of these nanotransducers nearly impossible, we have found simple rules for the design of effective wireless Joule nanoheaters. Moreover, we have shown that, if all aspect ratios are kept constant and the interface thermal conductivities are enough small, the downscaling of wireless Joule heaters does not degrade the *maximum* ΔT (this is an important result for *in vivo* biomedical applications where only very small ring-shaped structures could be used). Furthermore, we have discussed the potential use of wireless Joule nanoheaters for targeted drug delivery and hyperthermia. Finally, as an example, we have applied the results of our analysis to the design of multi-shell two layers wireless Joule nanoheaters based on zinc oxide nanorings.

Acknowledgments

Thanks to Dr. Cherif Ould Lahoucine, Prof. Fernando Bardati, Prof. Paolo Ferrazzoli, Prof. Gaetano Marrocco, Prof. Mario Salerno, Dr. Eugenio Martinelli, and Andrea Mauri for valuable discussions. The authors acknowledge MIUR (Ministero dell'Università e Ricerca, Italy) for supporting exchange visits between the University of Tor Vergata (Rome, Italy) and the Georgia Institute of Technology (Atlanta, GA) through the grant MIUR Interlink ("Esplorazione delle possibilità applicative di nano-strutture di ossido di zinco per la realizzazione di nano-sensori e nano-attuatori wire-less biocompatibili").

References

[1] C. Falconi, A. D'Amico, Z.L. Wang, Wireless nanosensors and nanoactuators for in-vivo biomedical applications, in: Proceedings of the Eurosensors XX, Goteborg, Sweden, 2006.
[2] A. Jordan, P. Wust, R. Scholz, B. Tesche, H. Fähling, T. Mitrovics, T. Vogl, J. Cervòs-Navarro, R. Felix, Cellular uptake of magnetic fluid particles and their effects on human adenocarcinoma cells exposed to AC magnetic fields in vitro, Int. Hypertherm. 12 (1996) 705.
[3] A. Jordan, R. Scholz, P. Wust, H. Fahling, R. Felix, Magnetic fluid hyperthermia (MFH): cancer treatment with AC magnetic field induced excitation of biocompatible superparamagnetic nanoparticles, J. Magn. Magn. Mater. 201 (1999) 413–419.
[4] C.C. Berry, A.S.G. Curtis, Functionalisation of magnetic nanoparticles for applications in biomedicine, J. Phys. D: Appl. Phys. 36 (2003) R198–R206.
[5] C. Loo, A. Lin, L. Hirsch, M.H. Lee, J. Barton, N. Halas, J. West, R. Drezek, Nanoshell-enabled photonics-based imaging and therapy of cancer, Technol. Cancer Res. Treat. 3 (2004) 33–40.
[6] A.S. Lübbe, C. Alexiou, C. Bergemann, Clinical applications of magnetic drug targeting, J. Surg. Res. 95 (2001) 200–206.
[7] A.S. Lübbe, C. Bergemann, H. Riess, F. Schriever, P. Reichardt, K. Possinger, M. Matthias, B. Dorken, F. Herrmann, R. Gurtler, P. Hohenberger, N. Haas, R. Sohr, B. Sander, A.J. Lemker, D. Ohlendorf, W. Huhnt, D. Huhn, Clinical experiences with magnetic drug targeting: a phase I study with 4′-epidoxorubicin in 14 patients with advanced solid tumors, Cancer Res. 56 (20) (1996) 44686–44693.
[8] S.R. Sershen, S.L. Westcott, N.J. Halas, J.L. West, Temperature-sensitive polymer-nanoshell composites for photothermally modulated drug delivery, J. Biomed. Mater. Res. 51 (2000) 293–298.
[9] S.R. Sershen, J.L. West, S.L. Westcott, N.J. Halas, Nanoshell-polymer composites for photothermally modulated drug delivery, in: Proceedings of the CLEO, 2001.
[10] A. Pohl, A review of wireless SAW sensors, IEEE Trans. Ultrason. Ferroelectrics Frequency Control 47 (2) (2000) 317–332.
[11] M. Ferrari, Cancer nanotechnology: opportunities and challenges, Nat. Rev. Cancer 5 (2005) 161–171.
[12] R.F. Service, Nanotechnology takes aim at cancer, Science 310 (2005) 1132–1134.

[13] E.S. Kawasaki, A. Player, Nanotechnology, nanomedicine, and the development of new, effective therapies for cancer, Nanomed.: Nanotechnol. Biol. Med. I (2005) 101–109.
[14] D.A. LaVan, T. McGuire, R. Langer, Small scale systems for *in-vivo* drug delivery, Nat. Biotechnol. 21 (10) (2003) 1184–1191.
[15] B. Panchapakesan, Nanotechnology. Part 2. Tiny technology—tremendous therapeutic potential, Oncol. Issues (2003) 20–23.
[16] D.C. Sullivan, M. Ferrari, Nanotechnology and tumor imaging: seizing an opportunity, Molec. Imag. 3 (4) (2004) 364–369.
[17] S. Sengupta, D. Eavarone, I. Capila, G. Zhao, N. Watson, T. Kiziltepe, R. Sasisekharan, Temporal targeting of tumour cells and neovasculature with a nanoscale delivery system, Nature 436 (2005) 568–572.
[18] Z.W. Pan, Z.R. Dai, Z.L. Wang, Nanobelts of semiconducting oxides, Science 291 (2001) 1947–1949.
[19] X.Y. Kong, Y. Ding, R.S. Yang, Z.L. Wang, Single-crystal nanorings formed by epitaxial self-coiling of polar-nanobelts, Science 303 (2004) 1348–1351.
[20] P.X. Gao, Y. Ding, W. Mai, W.L. Hughes, C.S. Lao, Z.L. Wang, Conversion of zinc oxide nanobelts into superlattice-structured nanohelices, Science 309 (2005) 1700–1704.
[21] W.L. Hughes, Z.L. Wang, Controlled synthesis and manipulation of ZnO nanorings and nanobows, Appl. Phys. Lett. 86 (2005) 43106-1-3.
[22] J.E. Kennedy, High-intensity focused ultrasound in the treatment of solid tumors, Nature 5 (2005) 321–327.
[23] D.G. Cahill, W.K. Ford, K.E. Goodson, G.D. Mahan, A. Majumdar, H.J. Maris, R. Merlin, S.R. Phillpot, Nanoscale thermal transport, J. Appl. Phys. 93 (2) (2003) 793–818.
[24] D. Poulikakos, S. Arcidiacono, S. Maruyama, Molecular dynamics: simulation in nanoscale heat transfer: a review, Microscale Thermophys. Eng. 7 (2003) 181–206.
[25] S. Maruyama, Molecular dynamics methods in microscale heat transfer, in: G.F. Hewitt (Ed.), Heat Transfer & Fluid Flow in Microchannels, Begell House, 2004, pp. 1–32, Chapter 7.
[26] S. Huxtable, D.G. Cahill, S. Shenogin, L. Xue, R. Ozisik, P. Barone, M. Userey, M.S. Strano, G. Siddons, M. Shim, P. Keblinski, Interfacial heat flow in carbon nanotube suspensions, Nat. Mater. 2 (2003) 731–734.
[27] S. Shenogin, L. Xue, R. Ozisik, P. Keblinski, D.G. Cahill, Role of thermal boundary resistance on the heat flow in carbon nanotube composites, J. Appl. Phys. 95 (12) (2004) 8136–8144.
[28] O.M. Wilson, X. Hu, D.G. Cahill, P.V. Braun, Colloidal metal particles as probes of nanoscale thermal transport in fluids, Phys. Rev. B 66 (2002) 224301.
[29] R.M. Costescu, D.G. Cahill, F.H. Fabreguette, Z.A. Sechrist, S.M. George, Ultra-low thermal conductivity in W/Al_2O_3 nanolaminates, Science 303 (2004) 989–990.
[30] W.L. Zhou, J. He, J. Fang, T. Huynh, T.J. Kennedy, K.L. Stokes, C.J. O'Connor, Self-assembly of Fe–Pt nanoparticles into nanorings, J. Appl. Phys. 93 (10) (2003) 7340–7342.
[31] J. Aizpurua, P. Hanarp, D.S. Sutherland, M. Kall, G.W. Bryant, F.J. Garcıa de Abajo, Optical properties of gold nanorings, Phys. Rev. Lett. 90 (5) (2003) 057401.
[32] D. Jia, A. Goonewardene, Two-dimensional nanotriangle and nanoring arrays on silicon wafer, Appl. Phys. Lett. 88 (2006) 053105.
[33] F.Q. Zhu, D. Fan, X. Zhu, J.G. Zhu, R.C. Cammarata, C.L. Chien, Ultrahigh density arrays of ferromagnetic nanorings on macroscopic areas, Adv. Mater. 16 (2004) 23–24.
[34] C.A. Balanis, Antenna Theory. Analysis and Design, 2nd ed., John Wiley & Sons, 1997.
[35] K. Ellmer, Resistivity of polycrystalline zinc oxide films: current status and physical limits, J. Phys. D: Appl. Phys. 34 (2001) 3097–3108.

Biographies

Christian Falconi was born in Rome, Italy, 1973. He received the MSc (cum laude) and the PhD degrees in electronic engineering from the University of Tor Vergata, Rome, Italy, in, respectively, 1998 and 2001; as a part of his PhD program he visited the University of Linkoping (1 month), and TU Delft (7 months). In 2002, he has supervised the design of the electronic interface for the ST-Microelectronics DNA chip. Since 2002 Christian Falconi is assistant professor at the Department of Electronic Engineering, University of Tor Vergata, where he teaches Low Voltage Analog Electronics and Fundamental of Electronics. Since 2003 he has been visiting the Georgia Institute of Technology (10 months). He authored or co-authored 35 papers on international journals and conference proceedings. His research interests include electronic devices, analog circuits, electronic interfaces, sensors, microsystems, and nanosystems.

Arnaldo D'Amico received the Laurea degree in physics and electronic engineering from the University La Sapienza, Rome, Italy. For several years, he has been with the National Research Council (CNR) leading the Semiconductors Laboratory at the Solid State Electronic Institute, Rome. In 1986, he was appointed full professor of electronics at the University of L'Aquila, and, since 1990, he has been with the University of Rome Tor Vergata where he leads the Sensors and Microsystems Group and is full professor of electronics, Faculty of Engineering. He teaches courses on electronic devices, microsystems, and sensors. Currently, his main research activities are concerned with the development of physical and chemical sensors, low voltage electronics, noise, and advanced electronic devices. He is author of more than 450 papers in international journals and conference proceedings. He has been Chairman of several conferences on sensors, electronics, and noise and a member of the editorial board of the journals Sensors and Actuators A (physical) and Sensors and Actuators B (chemical). He served as Chairman of the Steering Committee of the Eurosensors conference series from 1999 to 2004. At the national level, he is Chairman of the National Society of Sensors and Microsystems (AISEM) and Director of the Institute of Acoustics "O. M. Corbino" of the National Research Council (CNR).

Zhong Lin Wang received the BS degree in applied physics from the Northwest Telecommunication Engineering Institute, China, in 1982, and the PhD degree in physics from the Arizona State University in 1987. Subsequently, he was visiting lecturer at the Department of Material Science & Engineering, The State University of New York at Stony Brook (September 1987–September 1988); research fellow at the Cavendish Laboratory, University of Cambridge, England (October 1988–October 1989); research fellow at the U.S. Department of Energy, Research Fellowship, Metals and Ceramics Division, Oak Ridge National Laboratory (November 1989–September 1990); research associate professor at the Metals and Ceramics Division, Oak Ridge National Laboratory and Department of Materials Science, the University of Tennessee (September 1990–April 1993); research scientist at the National Institute of Standards and Technology (December 1993–February 1995). Since March 1995 he is with the School of Materials Science and Engineering, Georgia institute of Technology, where he currently is Regents' Professor, COE Distinguished Professor, and Director of the Center for Nanostructure Characterization and Fabrication. Wang has published over 480 articles in peer-reviewed journals, which have defining influence on the field of nanotechnology as evidenced by high citation (>16,000 times) and impact factor (his h-index is 60). He is the world top 25 most cited authors in nanotechnology from 1992–2002. Among other achievements, Dr. Wang and his group have first reported nanobelts of semiconducting oxides; self-assembled, single-crystal nanorings and nanohelixes; and piezoelectric nanogenerators.